How to cite: *Angew. Chem. Int. Ed.* **2021**, *60*, 5283–5288
International Edition: doi.org/10.1002/anie.202016225
German Edition: doi.org/10.1002/ange.202016225

Gas Separation | Hot Paper

A MOF-based Ultra-Strong Acetylene Nano-trap for Highly Efficient C_2H_2/CO_2 Separation

Zheng Niu, Xili Cui, Tony Pham, Gaurav Verma, Pui Ching Lan, Chuan Shan, Huabin Xing, Katherine A. Forrest, Shanelle Suepaul, Brian Space, Ayman Nafady, Abdullah M. Al-Enizi, and Shengqian Ma**

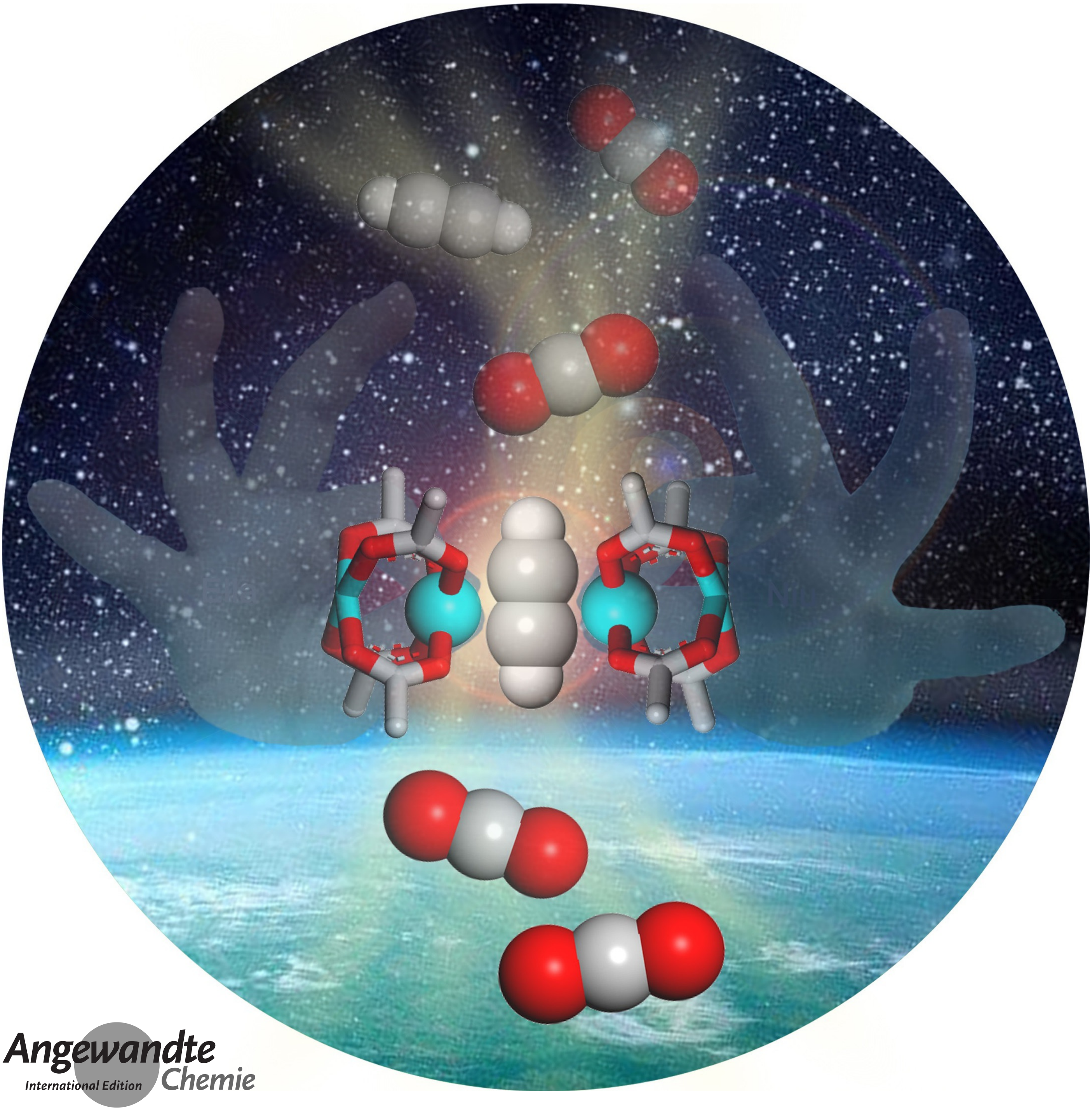

***Abstract:** Porous materials with open metal sites have been investigated to separate various gas mixtures. However, open metal sites show the limitation in the separation of some challenging gas mixtures, such as C_2H_2/CO_2. Herein, we propose a new type of ultra-strong C_2H_2 nano-trap based on multiple binding interactions to efficiently capture C_2H_2 molecules and separate C_2H_2/CO_2 mixture. The ultra-strong acetylene nano-trap shows a benchmark Q_{st} of 79.1 kJ mol^{-1} for C_2H_2, a record high pure C_2H_2 uptake of 2.54 mmol g^{-1} at 1×10^{-2} bar, and the highest C_2H_2/CO_2 selectivity (53.6), making it as a new benchmark material for the capture of C_2H_2 and the separation of C_2H_2/CO_2. The locations of C_2H_2 molecules within the MOF-based nanotrap have been visualized by the in situ single-crystal X-ray diffraction studies, which also identify the multiple binding sites accountable for the strong interactions with C_2H_2.*

Introduction

Gas separation and purification have attracted a widespread attention owing to that they account for a significant portion of the global energy consumption.[1] Presently, distillation technology is still playing a dictating role for separation and purification in the chemical industry, benefiting from its simple flowsheet and associated low capital investment.[2] However, the energy efficiency of distillation separation technology is very low, thereby leading to a remarkable energy consumption.[3] As a result of this limitation, adsorbent-based gas separation methods, including pressure swing adsorption (PSA), temperature swing adsorption (TSA), and membranes have attracted escalating interest owing to their high energy efficiency and intrinsic economic feasibility.[3,4]

The key to the adsorbent-based gas separation is the strong and abundant binding sites for the specific molecules in the porous materials. The conventional binding sites that focus on the isolated adsorption sites, which can be easily constructed, have shown great separation performance for various gas mixtures.[5] However, the weakness of the isolated adsorption sites is manifested in separating gas mixtures with similar size and physical properties. Compared with the isolated adsorption site, nano-trap with multiple adsorption sites provides stronger binding interaction and recognition capability for target molecules.[5d,6] As a crystalline porous material, metal-organic frameworks (MOFs) have emerged as a very promising platform for constructing nano-trap for specific molecules because of their tunable pore sizes and their functional pore environment.[7] In particular, the explicit single crystal structure of MOFs offers great opportunity to investigate the interaction mechanism for specific gases in nano-trap, which can facilitate the design of novel nano-trap for advanced separation.

In recent years, the MOF-based nano-traps or molecule traps have been developed to selectively capture specific gas molecules and separate gas mixtures.[5d,6] Although some nano-traps reveal inspiring separation performance in many gas mixtures, the powerful C_2H_2 nano-trap is scarce and challenging. As a significant starting material, C_2H_2 has been widely applied in the chemical industry.[8] However, the highly reactive acetylene may cause an undesirable chemical reaction in various industrial processes, and thus it must be separated.[9] The currently existing nanotraps exhibit insufficient binding capability for C_2H_2, thereby attesting the limited separation performance for challenging gas mixtures such as C_2H_2/CO_2, where the mixture components have very similar physical properties (boiling points: C_2H_2, 189.3 K; CO_2, 194.7 K) and almost identical kinetic diameters (ca. 3.3 Å).[10] In principle, increasing the binding interaction between the nano-trap and target gas molecules can effectively enhance the selective separation of the target molecule from the gas mixtures, therefore, a MOF with sufficiently strong C_2H_2 nanotrap would be a promising material for C_2H_2/CO_2 separation.

In this work, we proposed a new type of ultra-strong C_2H_2 nano-trap based on multiple binding interactions to efficiently capture C_2H_2 molecules and separate C_2H_2/CO_2 mixture. As shown in Scheme 1, the isosteric heat of adsorption (Q_{st}) of C_2H_2 for nano-trap adsorption site based on two SiF_6 (41.83 kJ mol^{-1} for SIFSIX-2-Cu-i) is much higher than single

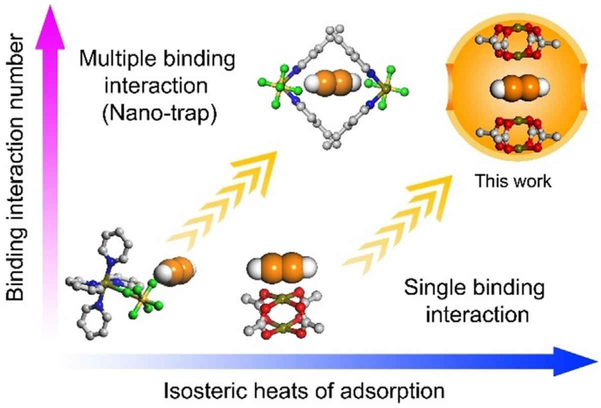

Scheme 1. The multiple interactions strategy for enhancing binding interaction between C_2H_2 and binding site.

---

[*] Dr. Z. Niu
College of Chemistry, Chemical Engineering and Materials Science
Soochow University, Suzhou 215123 (P. R. China)
E-mail: zhengniu@suda.edu.cn

Dr. G. Verma, P. C. Lan, Prof. S. Ma
Department of Chemistry, University of North Texas
Denton, TX 76201 (USA)
E-mail: Shengqian.Ma@unt.edu

T. Pham, C. Shan, Dr. K. A. Forrest, S. Suepaul, Prof. B. Space
Department of Chemistry, University of South Florida
4202 E. Fowler Avenue, Tampa, FL 33620 (USA)

Dr. X. Cui, Prof. H. Xing
Key Laboratory of Biomass Chemical Engineering of Ministry of Education, College of Chemical and Biological Engineering
Zhejiang University, Hangzhou 310027 (P. R. China)

Prof. A. Nafady, Prof. A. M. Al-Enizi
Department of Chemistry, College of Science, King Saud University
Riyadh 11451 (Saudi Arabia)

Supporting information and the ORCID identification number(s) for the author(s) of this article can be found under:
https://doi.org/10.1002/anie.202016225.

SiF_6 adsorption site (26.24 kJ mol^{-1} for SIFSIX-2-Cu).[11] Given that the Q_{st} of C_2H_2 for the open metal site is higher than SiF_6 ion adsorption site in MOFs,[12] we speculate that the nano-trap based on oppositely adjacent open metal sites would afford a much greater binding interaction with C_2H_2 than SiF_6 nano-trap, together with the record C_2H_2/CO_2 separation performance. In this regard, we choose an alkyl MOF, ATC-Cu, which features unique oppositely adjacent Cu-paddlewheel open metal sites, thereby increasing the energetic favorability toward C_2H_2 molecules. Taking advantage of the designed C_2H_2 nano-trap, the anhydrous ATC-Cu demonstrates the strongest C_2H_2 binding capability with the largest Q_{st} and the highest uptake amount at ultra-low pressure (< 0.001 bar), as well as the benchmark C_2H_2/CO_2 selectivity at room temperature.

Results and Discussion

The hydrothermal reaction of H_2ATC (1,3,5,7-adamantane tetracarboxylic acid) ligand and copper nitrate hydrate was employed to synthesize the ATC-Cu ($Cu_2(ATC)$);[13] experimental details are provided in SI. As shown in Figure 1, four Cu paddle-wheel secondary building units (SBUs) were connected by the ATC ligand to construct a 4,4-coordinated net. The rectangular channels established by the oppositely adjacent Cu-paddle wheels and aliphatic hydrocarbon cavities with a size of 4.43 × 5.39 Å (after subtracting van der Waals radius) can be observed along with *b* and *c* axes. The Cu-Cu distance between neighboring Cu paddlewheels is only 4.43 Å after subtracting van der Waals radius, thereby affording a considerable dual potential coordination interaction within this region and possibly generating a strong binding site for acetylene (Figure 1). Furthermore, the aliphatic hydrocarbon cavities in ATC-Cu features twelve inward hydrogen atoms with a short average distance (3.5 Å) between these hydrogen atoms and the center of the cavity provides another potential adsorption site for acetylene (Figure 1). The combination of aliphatic hydrocarbon low polarity cavities and the oppositely adjacent unsaturated metal sites endows ATC-Cu with the potential for ultra-high acetylene binding affinity and high uptake amount. The PXRD pattern of the as-synthesized ATC-Cu sample agrees well with the calculated pattern obtained from the single crystal data. Meanwhile, the TAG data revealed that ATC-Cu is stable till 270 °C. The ATC-Cu has a Brunauer–Emmett–Teller (BET) surface area of 600 m^2 g^{-1} (Langmuir surface area: 667 m^2 g^{-1}) calculated from the N_2 sorption isotherms at 77 K.

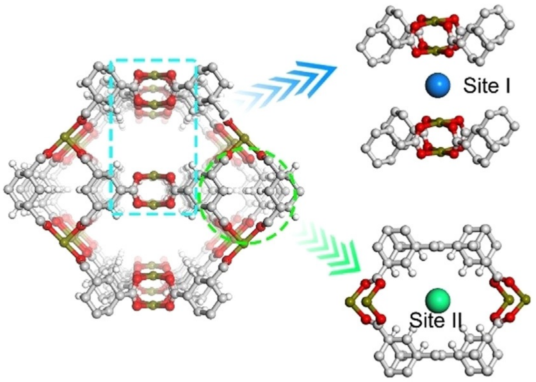

Figure 1. The channel structure of ATC-Cu and the primary two C_2H_2 binding site in the framework.

The single-component adsorption isotherms for C_2H_2 and CO_2 were collected for ATC-Cu at 273 K and 298 K (Figure 2 a). ATC-Cu was found to adsorb 5.01 mmol g^{-1} of C_2H_2 at 298 K and 1 bar, which shows markedly high C_2H_2 uptake capability. In contrast, the CO_2 uptake amount of ATC-Cu is only 4.02 mmol g^{-1} at 298 K and 1 bar. Significantly, the value of the C_2H_2 uptake amount for ATC-Cu at ultra-low pressure (1×10^{-3} bar) reaches to 2.1 mmol g^{-1}, which is the highest value among all of the reported acetylene adsorbent materials and much higher than CO_2 uptake amount for ATC-Cu at the same condition (0.3 mmol g^{-1} at room temperature and 1×10^{-3} bar). As illustrated in Figure 2 b, ATC-Cu shows the remarkable C_2H_2 adsorption capability with the highest uptake amount at 298 K/1×10^{-2} bar (Supporting Information, Table S3) compared with other high-performance C_2H_2 adsorbents, including SIFSIX-2-Cu-i,[11a] HKUST-1,[12a] Ni-MOF-74,[12b] SIFSIX-2-Cu,[11a] NKMOF-Ni-1,[14] FeNiM′ MOF,[15] ZJU-74,[16] DICRO-4-Ni-i,[17] and JCM-1.[18]

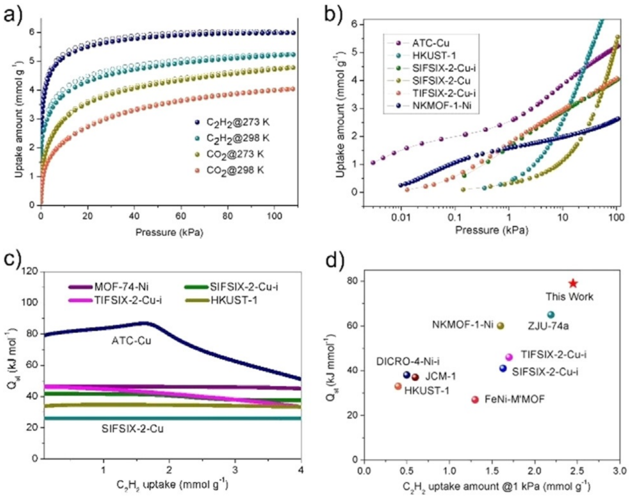

Figure 2. a) The C_2H_2 and CO_2 isotherms for ATC-Cu at 273 K and 298 K. b) The C_2H_2 adsorption isotherms for ATC-Cu and high performed MOFs at 298 K. c) The Q_{st} for ATC-Cu and high performed MOFs. d) The Q_{st} against C_2H_2 uptake amount at 1×10^{-2} bar for high-performance acetylene adsorbent.

The Q_{st} of C_2H_2 and CO_2 in the ATC-Cu were calculated based on the mathematical analysis of the gas adsorption isotherms at two different temperatures to investigate the interaction strength between the gases and the framework. The C_2H_2 isotherm data at 298, 313, and 333 K, and CO_2 isotherm data at 273 and 298 K were fitted to the dual-site Langmuir-Freundlich (DSLF) equation, and the Q_{st} values were subsequently calculated using the Clausius–Clapeyron equation (see the Supporting Information). As shown in Figure 2c, the zero-coverage Q_{st} value for C_2H_2 in ATC-Cu (79.1 kJ mol^{-1}) is significantly higher than all of the high-performance MOFs with isolated binding sites and multiple binding sites, such as MOF-74-Ni (45 kJ mol^{-1}) and HKUST-1 (30.4 kJ mol^{-1}), implying an unusual strong binding interaction between acetylene and ATC-Cu. Notably, the Q_{st} value for C_2H_2 loading in ATC-Cu reaches to 80 kJ mol^{-1}, which is also higher than current benchmark materials. As presented in Figure 2d, ATC-Cu shows the benchmark Q_{st} and uptake amount at low pressure for C_2H_2 compared to the currently existing high-performance C_2H_2 adsorbents.

The theoretical studies utilizing preliminary grand canonical Monte Carlo (GCMC) simulations and periodic density functional theory (DFT) calculations were employed to investigate the unprecedented acetylene adsorption performance of ATC-Cu. Based on the calculation results, there are two primary binding sites (Site I and site II) for acetylene found in ATC-Cu. Site I is located in the middle of two oppositely adjacent Cu-paddle wheels, while Site II is located in the aliphatic hydrocarbon cavity enclosed by four neighboring ATC linkers. As expected, the proximity of two unsaturated metal sites on oppositely neighboring Cu paddlewheels affords an acetylene nano-trap with dual coordination interaction, thereby generating a super strong binding site for acetylene. A static adsorption energy was calculated to be 64.35 kJ mol^{-1} for the Site I, which confirms the strong interaction between the oppositely adjacent open metal sites and acetylene molecule. Compared with site I, the primary interaction for acetylene on the Site II is multiple van der Waals interactions with the nearby framework H atoms.

To visualize the locations of acetylene molecules in ATC-Cu and elucidate the its binding affinity for acetylene, we carried out the in situ single-crystal X-ray diffraction (SCXRD) experiment. The acetylene loaded ATC-Cu crystals (C_2H_2@ATC-Cu) were prepared at room temperature and different acetylene pressures (1×10^{-4} bar and 1 bar). The SCXRD data of C_2H_2@ATC-Cu (CCDC Number: 2052339)[19] at very low pressure (1×10^{-4} bar) revealed the strongest C_2H_2 binding site in ATC-Cu. As presented in Figure 3b, the C_2H_2 molecule was located in the middle of the oppositely adjacent Cu-paddle wheels at very low pressure (1×10^{-4} bar), consistent with the primary binding site (site I) determined by the modeling studies. The distance between the acetylene molecule and the adjacent open metal site (C-Cu) is 2.9 Å, which is larger than the reported value but shows an unexpected strong binding interaction because of the duel coordination interactions. The SCXRD data indicates that ATC-Cu adsorbed one C_2H_2 molecule per unit cell at 1×10^{-4} bar, which corresponds to 2.23 mmol g^{-1} of C_2H_2 uptake amount and is consistent with the experimental gas adsorption data for ATC-Cu. After increasing the pressure of C_2H_2 to 1 bar, the acetylene molecules filled the aliphatic hydrocarbon cavity (site II), and other acetylene molecules distribute into the channels close to the site I. The in situ SCXRD studies suggest that at room temperature C_2H_2 molecule can be preferentially trapped by nanotrap in ATC-Cu at very low pressure, and then binding to other adsorption sites with the C_2H_2 pressure increased. The experimental 2.3 mmol loading Q_{st} is close to the static adsorption energy that was calculated about Site I through periodic DFT calculations.

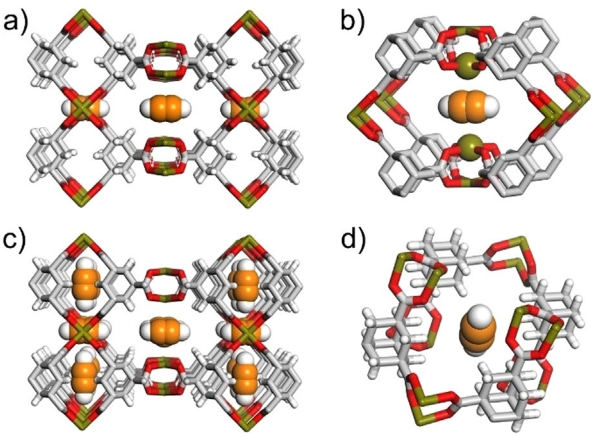

Figure 3. The SCXRD determined the location of C_2H_2 a) in the framework of ATC-Cu and b) on the Site I at 1×10^{-4} bar, and in the framework of ATC-Cu and c) on the Site II d) at 1 bar (CCDC Number: 2052340).[19]

Prompted by the significant difference in the uptake amount at very low pressure and the Q_{st} between C_2H_2 and CO_2 in ATC-Cu (Supporting Information, Figures S8 and S9), the C_2H_2/CO_2 selectivity was calculated using ideal adsorbed solution theory (IAST) to evaluate the potential of ATC-Cu for separating C_2H_2/CO_2. As displayed in Figure 4a, the calculated C_2H_2/CO_2 selectivity for the corresponding binary equimolar mixture in ATC-Cu is up to 53.6 at 298 K and 1 bar, which is much higher than the current benchmark, ZJU-74a (36.5). The IAST calculation revealed that the combination of the oppositely adjacent-open metal site and alkane cavity can bestow a MOF material with both high productivity and exceptional selectivity for acetylene from C_2H_2/CO_2 gas mixture.

To further evaluate the C_2H_2/CO_2 separation performance of ATC-Cu in practical adsorption processes, breakthrough experiments for C_2H_2/CO_2 at 298 K were conducted. The C_2H_2/CO_2 mixture gases flowed over a packed column of activated ATC-Cu with a rate of 2 mL per min. For C_2H_2/CO_2 (50:50, v/v) complete separation of C_2H_2 from mixtures can be realized by using activated ATC-Cu. As presented in Figure 4b, CO_2 breakthrough occurred at 213 min for C_2H_2/

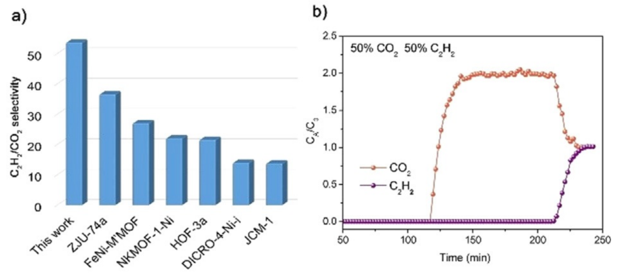

Figure 4. a) The C_2H_2/CO_2 selectivity of ATC-Cu and reported high-performance MOFs at 298 K and 1 bar. b) The experimental breakthrough curve for C_2H_2/CO_2 at 298 K.

CO_2 (50:50). These results illustrate that ATC-Cu is highly efficient for the demanding separation of C_2H_2/CO_2 mixtures at normal pressure and temperature.

Conclusion

We report an ultra-strong acetylene nano-trap based on the oppositely adjacent open metal sites in MOFs. This unique acetylene nano-trap showed the strongest binding interaction with C_2H_2 in presently available porous materials, with a benchmark Q_{st} (79.1 kJ mol^{-1}). The mechanistic aspects of the binding process of ATC-Cu for the acetylene has been illustrated via acetylene loaded SCXRD studies along with theoretical calculations. The combined results clearly established that this new type of ultra-strong acetylene nano-trap can provide very strong binding interaction for acetylene at very low pressure. Significantly, the MOF-based acetylene nano-trap of ATC-Cu fosters a record high pure C_2H_2 uptake at 1×10^{-2} bar in pure C_2H_2 and in a binary equimolar C_2H_2/CO_2 mixture at 298 K and 1 bar, as well as the highest C_2H_2/CO_2 selectivity, making it as a new benchmark material for the capture of C_2H_2 and the separation of C_2H_2/CO_2. As a major outcome, this work offers a new platform to design and implement novel porous materials with ultra-strong binding affinity for C_2H_2, thereby attesting the significant role of MOFs in resolving industrial and environmental challenges.

Acknowledgements

The authors thank the support from the US National Science Foundation (DMR-1352065) and the Robert A. Welch Foundation (B-0027). Z.N. acknowledges the National Natural Science Foundation of China (Grant No. 22001186) and the Natural Science Foundation of Jiangsu Province (Grant No. BK20200853). T.P., K.A.F., and B.S. acknowledges the National Science Foundation (Award No. DMR-1607989), including support from the Major Research Instrumentation Program (Award No. CHE-1531590). Computational resources were made available by a XSEDE Grant (No. TG-DMR090028) and by Research Computing at the University of South Florida. B.S. also acknowledges support from an ACS Petroleum Research Fund grant (ACS PRF 56673-ND6). The authors also extend their appreciation to Researchers Supporting Program (RSP-2021/55) at King Saud University, Riyadh, Saudi Arabia for partial funding of this work.

Conflict of interest

The authors declare no conflict of interest.

Keywords: acetylene nano-trap · C_2H_2/CO_2 separation · in situ single-crystal X-ray diffraction · MOFs

---

[1] D. S. Sholl, R. P. Lively, *Nature* **2016**, *532*, 435 – 437.

[2] S. Chu, Y. Cui, N. Liu, *Nat. Mater.* **2017**, *16*, 16 – 22.

[3] R.-B. Lin, S. Xiang, W. Zhou, B. Chen, *Chem* **2020**, *6*, 337 – 363.

[4] a) S. Sircar, *Ind. Eng. Chem. Res.* **2002**, *41*, 1389 – 1392; b) X. Zhao, Y. Wang, D.-S. Li, X. Bu, P. Feng, *Adv. Mater.* **2018**, *30*, 1705189; c) Z.-G. Gu, J. Zhang, *Coord. Chem. Rev.* **2019**, *378*, 513 – 532.

[5] a) H. Yang, F. Peng, C. Dang, Y. Wang, D. Hu, X. Zhao, P. Feng, X. Bu, *J. Am. Chem. Soc.* **2019**, *141*, 9808 – 9812; b) E. D. Bloch, L. J. Murray, W. L. Queen, S. Chavan, S. N. Maximoff, J. P. Bigi, R. Krishna, V. K. Peterson, F. Grandjean, G. J. Long, B. Smit, S. Bordiga, C. M. Brown, J. R. Long, *J. Am. Chem. Soc.* **2011**, *133*, 14814 – 14822; c) Y.-S. Bae, C. Y. Lee, K. C. Kim, O. K. Farha, P. Nickias, J. T. Hupp, S. T. Nguyen, R. Q. Snurr, *Angew. Chem. Int. Ed.* **2012**, *51*, 1857 – 1860; *Angew. Chem.* **2012**, *124*, 1893 – 1896; d) G. L. Smith, J. E. Eyley, X. Han, X. Zhang, J. Li, N. M. Jacques, H. G. W. Godfrey, S. P. Argent, L. J. McCormick McPherson, S. J. Teat, Y. Cheng, M. D. Frogley, G. Cinque, S. J. Day, C. C. Tang, T. L. Easun, S. Rudić, A. J. Ramirez-Cuesta, S. Yang, M. Schröder, *Nat. Mater.* **2019**, *18*, 1358 – 1365.

[6] a) L. Yang, X. Cui, Q. Yang, S. Qian, H. Wu, Z. Bao, Z. Zhang, Q. Ren, W. Zhou, B. Chen, H. Xing, *Adv. Mater.* **2018**, *30*, 1705374; b) M. Wriedt, J. P. Sculley, A. A. Yakovenko, Y. Ma, G. J. Halder, P. B. Balbuena, H.-C. Zhou, *Angew. Chem. Int. Ed.* **2012**, *51*, 9804 – 9808; *Angew. Chem.* **2012**, *124*, 9942 – 9946; c) O. T. Qazvini, R. Babarao, Z.-L. Shi, Y.-B. Zhang, S. G. Telfer, *J. Am. Chem. Soc.* **2019**, *141*, 5014 – 5020; d) Z. Niu, X. Cui, T. Pham, P. C. Lan, H. Xing, K. A. Forrest, L. Wojtas, B. Space, S. Ma, *Angew. Chem. Int. Ed.* **2019**, *58*, 10138 – 10141; *Angew. Chem.* **2019**, *131*, 10244 – 10247; e) H.-G. Hao, Y.-F. Zhao, D.-M. Chen, J.-M. Yu, K. Tan, S. Ma, Y. Chabal, Z.-M. Zhang, J.-M. Dou, Z.-H. Xiao, G. Day, H.-C. Zhou, T.-B. Lu, *Angew. Chem. Int. Ed.* **2018**, *57*, 16067 – 16071; *Angew. Chem.* **2018**, *130*, 16299 – 16303; f) X. Cui, Q. Yang, L. Yang, R. Krishna, Z. Zhang, Z. Bao, H. Wu, Q. Ren, W. Zhou, B. Chen, H. Xing, *Adv. Mater.* **2017**, *29*, 1606929; g) L. Yang, L. Yan, Y. Wang, Z. Liu, J. He, Q. Fu, D. Liu, X. Gu, P. Dai, L. Li, X. Zhao, *Angew. Chem. Int. Ed.* **2020**, https://doi.org/10.1002/anie.202013965; *Angew. Chem.* **2020**,#https://doi.org/10.1002/ange.202013965.

[7] a) Q.-G. Zhai, X. Bu, X. Zhao, D.-S. Li, P. Feng, *Acc. Chem. Res.* **2017**, *50*, 407 – 417; b) J. Yu, L.-H. Xie, J.-R. Li, Y. Ma, J. M. Seminario, P. B. Balbuena, *Chem. Rev.* **2017**, *117*, 9674 – 9754; c) K. Adil, Y. Belmabkhout, R. S. Pillai, A. Cadiau, P. M. Bhatt, A. H. Assen, G. Maurin, M. Eddaoudi, *Chem. Soc. Rev.* **2017**, *46*, 3402 – 3430; d) D. Banerjee, A. J. Cairns, J. Liu, R. K. Motkuri, S. K. Nune, C. A. Fernandez, R. Krishna, D. M. Strachan, P. K. Thallapally, *Acc. Chem. Res.* **2015**, *48*, 211 – 219; e) Q. Yang, D. Liu, C. Zhong, J.-R. Li, *Chem. Rev.* **2013**, *113*, 8261 – 8323; f) J.-R. Li, J. Sculley, H.-C. Zhou, *Chem. Rev.* **2012**, *112*, 869 – 932; g) J.-R. Li, Y. Ma, M. C. McCarthy, J. Sculley, J. Yu, H.-K. Jeong, P. B. Balbuena, H.-C. Zhou, *Coord. Chem. Rev.* **2011**, *255*, 1791 – 1823; h) R.-B. Lin, H. Wu, L. Li, X.-L. Tang, Z. Li, J. Gao, H. Cui, W. Zhou, B. Chen, *J. Am. Chem. Soc.* **2018**, *140*, 12940 – 12946; i) M. K. Taylor, T. Runčevski, J. Oktawiec, J. E. Bachman, R. L. Siegelman, H. Jiang, J. A. Mason, J. D. Tarver, J. R. Long, *J. Am. Chem. Soc.* **2018**, *140*, 10324 – 10331; j) H. Jiang, J. Jia, A. Shkurenko, Z. Chen, K. Adil, Y. Belmabkhout, L. J. Weselinski, A. H. Assen, D.-X. Xue, M. O'Keeffe, M. Eddaoudi, *J. Am. Chem. Soc.* **2018**, *140*, 8858 – 8867; k) Z. Bao, D. Xie, G. Chang, H. Wu, L. Li, W. Zhou, H. Wang, Z. Zhang, H. Xing, Q. Yang, M. J. Zaworotko, Q. Ren, B. Chen, *J. Am. Chem. Soc.* **2018**, *140*, 4596 – 4603; l) J. E. Bachman, M. T. Kapelewski, D. A. Reed, M. I. Gonzalez, J. R. Long, *J. Am. Chem. Soc.* **2017**, *139*, 15363 – 15370; m) D. O'Nolan, A. Kumar, M. J. Zaworotko, *J. Am. Chem. Soc.* **2017**, *139*, 8508 – 8513; n) R.-B. Lin, L. Li, H. Wu, H.

Arman, B. Li, R.-G. Lin, W. Zhou, B. Chen, *J. Am. Chem. Soc.* **2017**, *139*, 8022 – 8028.

[8] P. Pässler, W. Hefner, K. Buckl, H. Meinass, A. Meiswinkel, H.-J. Wernicke, G. Ebersberg, R. Müller, J. Bässler, H. Behringer, D. Mayer, *Ullmann's Encyclopedia of Industrial Chemistry*, Wiley-VCH, Weinheim, **2000**.

[9] a) A. Granada, S. B. Karra, S. M. Senkan, *Ind. Eng. Chem. Res.* **1987**, *26*, 1901 – 1905; b) R. Matsuda, R. Kitaura, S. Kitagawa, Y. Kubota, R. V. Belosludov, T. C. Kobayashi, H. Sakamoto, T. Chiba, M. Takata, Y. Kawazoe, Y. Mita, *Nature* **2005**, *436*, 238 – 241.

[10] C. R. Reid, K. M. Thomas, *J. Phys. Chem. B* **2001**, *105*, 10619 – 10629.

[11] a) X. Cui, K. Chen, H. Xing, Q. Yang, R. Krishna, Z. Bao, H. Wu, W. Zhou, X. Dong, Y. Han, B. Li, Q. Ren, M. J. Zaworotko, B. Chen, *Science* **2016**, *353*, 141; b) K.-J. Chen, H. S. Scott, D. G. Madden, T. Pham, A. Kumar, A. Bajpai, M. Lusi, K. A. Forrest, B. Space, J. J. Perry, M. J. Zaworotko, *Chem* **2016**, *1*, 753 – 765.

[12] a) S. Xiang, W. Zhou, J. M. Gallegos, Y. Liu, B. Chen, *J. Am. Chem. Soc.* **2009**, *131*, 12415 – 12419; b) F. Luo, C. Yan, L. Dang, R. Krishna, W. Zhou, H. Wu, X. Dong, Y. Han, T.-L. Hu, M. O'Keeffe, L. Wang, M. Luo, R.-B. Lin, B. Chen, *J. Am. Chem. Soc.* **2016**, *138*, 5678 – 5684.

[13] B. Chen, M. Eddaoudi, T. M. Reineke, J. W. Kampf, M. O'Keeffe, O. M. Yaghi, *J. Am. Chem. Soc.* **2000**, *122*, 11559 – 11560.

[14] Y.-L. Peng, T. Pham, P. Li, T. Wang, Y. Chen, K.-J. Chen, K. A. Forrest, B. Space, P. Cheng, M. J. Zaworotko, Z. Zhang, *Angew. Chem. Int. Ed.* **2018**, *57*, 10971 – 10975; *Angew. Chem.* **2018**, *130*, 11137 – 11141.

[15] J. Gao, X. Qian, R.-B. Lin, R. Krishna, H. Wu, W. Zhou, B. Chen, *Angew. Chem. Int. Ed.* **2020**, *59*, 4396 – 4400; *Angew. Chem.* **2020**, *132*, 4426 – 4430.

[16] J. Pei, K. Shao, J.-X. Wang, H.-M. Wen, Y. Yang, Y. Cui, R. Krishna, B. Li, G. Qian, *Adv. Mater.* **2020**, *32*, 1908275.

[17] H. S. Scott, M. Shivanna, A. Bajpai, D. G. Madden, K.-J. Chen, T. Pham, K. A. Forrest, A. Hogan, B. Space, J. J. Perry IV, M. J. Zaworotko, *ACS Appl. Mater. Interfaces* **2017**, *9*, 33395 – 33400.

[18] J. Lee, C. Y. Chuah, J. Kim, Y. Kim, N. Ko, Y. Seo, K. Kim, T. H. Bae, E. Lee, *Angew. Chem. Int. Ed.* **2018**, *57*, 7869 – 7873; *Angew. Chem.* **2018**, *130*, 7995 – 7999.

[19] Deposition Numbers 2052339 and 2052340 contain the supplementary crystallographic data for this paper. These data are provided free of charge by the joint Cambridge Crystallographic Data Centre and Fachinformationszentrum Karlsruhe Access Structures service www.ccdc.cam.ac.uk/structures.

Manuscript received: December 6, 2020
Accepted manuscript online: January 6, 2021
Version of record online: February 4, 2021